Electrochemical Stability of Thin-Film $LiCoO_2$ Cathodes by Aluminum-Oxide Coating

Yong Jeong Kim,*,† Hyemin Kim,† Byoungsoo Kim,† Donggi Ahn,† Joon-Gon Lee,† Tae-Joon Kim,† Dongyeon Son,† Jaephil Cho,‡ Young-Woon Kim,† and Byungwoo Park*,†

School of Materials Science and Engineering, and Research Center for Energy Conversion and Storage, Seoul National University, Seoul, Korea, and Department of Applied Chemistry, Kumoh National Institute of Technology, Gumi, Korea

Received November 21, 2002

High-performance thin-film $LiCoO_2$ cathodes were successfully fabricated by aluminum-oxide coating. Both the galvanostatic charge−discharge experiments and the cyclic voltammograms (CVs) showed enhanced electrochemical properties in the Al_2O_3-coated $LiCoO_2$ films compared to those in the uncoated ones. The improved cycling behaviors in the coated samples are caused by the suppression of cobalt dissolution from the $LiCoO_2$ thin films, with the formation of an aluminum-oxide solid electrolyte residing between the $LiCoO_2$ cathode and liquid electrolyte. Galvanostatic intermittent titration technique (GITT) results clearly showed that the Al_2O_3-coated samples had higher Li diffusivities than the uncoated ones after 80 cycles. The effect of Al_2O_3 thickness on the electrochemical properties up to 300 nm was also studied.

Introduction

$LiCoO_2$ cathode materials have been studied extensively because of their excellent electrochemical properties and the ease of synthesizing a hexagonal α-$NaFeO_2$ structure, where alternating planes containing Li and Co ions are separated by close-packed oxygen layers.[1−4] Fabricating these materials as thin-film cathodes for all-solid-state microbatteries has been a major focus of research. This is due to the need to miniaturize various electronic devices, such as the monolithic hybridization with CMOS−RAM, back-up power systems for computer chips, small sensors, and hazard cards.[5−8] Thin-film cathodes have also received much attention due to the intrinsic electrochemical properties of lithiated transition-metal oxides, and because composite powders with polymer binders and carbon blacks may not represent the characteristic electrochemical properties of these oxides.[7−17]

$LiCoO_2$ cathode materials are typically charged up to ∼4.2 V vs Li ($Li_{0.5}CoO_2$), yielding a specific capacity below ∼140 mAh/g. Additional Li ions can be extracted from $Li_{0.5}CoO_2$ by raising the charge cutoff voltage. However, overcharging is often found to cause significant deterioration in the stability of $LiCoO_2$ due to a monoclinic to hexagonal ($M \rightarrow H$) phase transition, which induces extended defects (microcracks) between and within the particles,[1−3] and potential surface reactions such as cobalt dissolution above 4.4 V.[4] Recently, Cho et al.[18−22] reported that a thin-film metal-oxide coating (Al_2O_3, ZrO_2, etc.) on the surface of $LiCoO_2$ powders showed excellent capacity retention even at the cutoff voltage of 4.4 V. However, the mechanisms for the effect of metal-oxide coating have not yet been clearly identified.

* Authors to whom correspondence should be addressed. E-mail: sanmaro1@snu.ac.kr. or byungwoo@snu.ac.kr.
† Seoul National University.
‡ Kumoh National Institute of Technology.

(1) Reimers, J. N.; Dahn, J. R. *J. Electrochem. Soc.* **1992**, *139*, 2091.
(2) Ohzuku, T.; Ueda, A. *J. Electrochem. Soc.* **1944**, *141*, 2972.
(3) Wang, H.; Jang, Y.-I.; Huang, B.; Sadoway, D. R.; Chiang, Y.-M. *J. Electrochem. Soc.* **1999**, *146*, 473.
(4) Amatucci, G. G.; Tarascon, J. M.; Klein, L. C. *Solid State Ionics* **1996**, *83*, 167.
(5) Wolverton, C.; Zunger, A. *J. Electrochem. Soc.* **1998**, *145*, 2424.
(6) Fauteux, D. G.; Massucco, A.; Shi, J.; Lampe-Onnerud, C. *J. Appl. Electrochem.* **1997**, *27*, 543.
(7) Wang, B.; Bates, J. B.; Hart, F. X.; Sales, B. C.; Zuhr, R. A.; Robertson, J. D. *J. Electrochem. Soc.* **1996**, *143*, 3203.
(8) Bates, J. B.; Dudney, N. J.; Neudecker, B. J.; Hart, F. X.; Jun, H. P.; Hackney, S. A. *J. Electrochem. Soc.* **2000**, *147*, 59.
(9) Antaya, M.; Dahn, J. R.; Preston, J. S.; Rossen, E.; Reimers, J. N. *J. Electrochem. Soc.* **1993**, *140*, 575.
(10) Jang, Y.-I.; Neudecker, B. J.; Dudney, N. J. *Electrochem. Solid-State Lett.* **2001**, *4*, A74.
(11) Lee, J.-K.; Lee, S.-J.; Baik, H.-K.; Lee, H.-Y.; Jang, S.-W.; Lee, S.-M. *Electrochem. Solid-State Lett.* **1999**, *2*, 512.
(12) Striebel, K. A.; Deng, C. Z.; Wen, S. J.; Cairns, E. J. *J. Electrochem. Soc.* **1996**, *143*, 1821.
(13) Iriyama, Y.; Inaba, M.; Abe, T.; Ogumi, Z. *J. Power Sources* **2001**, *94*, 175.
(14) Perkins, J. D.; Bahn, C. S.; McGraw, J. M.; Parilla, P. A.; Ginley, D. S. *J. Electrochem. Soc.* **2001**, *148*, A1302.
(15) Bouwman, P. J.; Boukamp, B. A.; Bouwmeester, H. J. M.; Notten, P. H. L. *J. Electrochem. Soc.* **2002**, *149*, A699.
(16) Perkins, J. D.; Bahn, C. S.; Parilla, P. A.; McGraw, J. M.; Fu, M. L.; Duncan, M.; Yu, H.; Ginley, D. S. *J. Power Sources* **1999**, *81*−*82*, 675.
(17) Kim, Y. J.; Kim, T.-J.; Shin, J. W.; Park, B.; Cho, J. *J. Electrochem. Soc.* **2002**, *149*, A1337.
(18) Cho, J.; Kim, Y. J.; Park, B. *Chem. Mater.* **2000**, *12*, 3788.
(19) Cho, J.; Kim, Y. J.; Kim, T.-J.; Park, B. *Angew. Chem., Int. Ed.* **2001**, *40*, 3367.
(20) Cho, J.; Kim, Y. J.; Park, B. *J. Electrochem. Soc.* **2001**, *148*, A1110.
(21) Cho, J.; Kim, Y. J.; Kim, T.-J.; Park, B. *Chem. Mater.* **2001**, *13*, 18.
(22) Kim, Y. J.; Cho, J.; Kim, T.-J.; Park, B. *Electrochem. Solid-State Lett.* submitted for publication.

10.1021/cm0201403 CCC: $25.00 © 2003 American Chemical Society
Published on Web 03/15/2003

In this paper, a novel coating technology for improving the cycle-life performance in thin-film $LiCoO_2$ cathodes is reported. The effect of Al_2O_3 coating on cobalt dissolution from the $LiCoO_2$ films is investigated, and the Li diffusivities are determined during a Li intercalation and deintercalation. The Al_2O_3 coating thicknesses are also varied from 10 to 300 nm to determine the effects on the electrochemical properties.

Experimental Section

The $LiCoO_2$ thin films (1 cm^2) were deposited on thermally oxidized SiO_2/Si (100) substrates by rf magnetron sputtering using a stoichiometric $LiCoO_2$ target (2-in. diam.). The target was fabricated by cold-pressing commercial $LiCoO_2$ powders followed by sintering at 1000 °C for 10 h in air. A Pt current collector was deposited prior to the $LiCoO_2$ film deposition. To improve the Pt adhesion to the substrate, a TiO_2 underlayer was deposited by the reactive sputtering of Ti. $LiCoO_2$ thin-film deposition was conducted at a pressure of 20 mTorr with an Ar/O_2 ratio of 3:1 after presputtering for 1 h. The deposition rate was ~2 nm/min with an rf power of 100 W, and a ~600-nm-thick film was deposited. To obtain good-quality $LiCoO_2$ thin films, all rf-sputtered films were annealed at 700 °C in an oxygen atmosphere of 10 mTorr for 30 min. The Al_2O_3 thin films were deposited on top of the crystallized $LiCoO_2$ films by the reactive sputtering of an Al target. After Al_2O_3 deposition, the coated samples were heat-treated at 400 °C for 5 h in flowing oxygen.

The structural characterization of $LiCoO_2$ films was performed by X-ray diffraction (XRD) and transmission electron microscopy (TEM). The film composition and depth profile near the Al_2O_3-coated film surface were obtained using inductively coupled plasma−atomic emission spectroscopy (ICP−AES) and Auger electron spectroscopy (AES), respectively. The interface between the aluminum-oxide layer and $LiCoO_2$ was also characterized by energy-dispersive X-ray spectroscopy (EDS) in TEM.

The electrochemical characteristics of the $LiCoO_2$ thin films were investigated using both galvanostatic charge−discharge experiments and cyclic voltammograms (CVs). Beaker-type half-cells were used to characterize the electrochemical properties of both the uncoated and Al_2O_3-coated $LiCoO_2$ thin films. The electrochemical cells consisted of Li-metal sheets as a counter and reference electrode, a $LiCoO_2$ film of approximately 1 cm^2 of active area as the working electrode, and 1 M $LiPF_6$ in EC/DEC (1/1 vol. %) (*Cheil Industries Inc.*) as the electrolyte. The cells were electrochemically cycled over the voltage range of 2.75 and 4.4 V with current rates of 0.2 and 0.4 mA/cm^2. At all the charge/discharge cutoff steps, the cell voltages were potentiostated until the current decreased to 10% of the charge/discharge rates. To determine the Li diffusivities as a function of the cell potential, a galvanostatic intermittent titration technique (GITT) with current steps of 0.4 mA/cm^2 for 10 s was used for both the uncoated and Al_2O_3-coated $Li_{1-x}CoO_2$ films. Ten minutes of equilibration were allowed between steps. CVs of both bare and Al_2O_3-coated $LiCoO_2$ films were recorded at a sweep rate of 0.1 mV/sec, during the first cycle, and after the 40th and 80th cycles at 0.2 mA/cm^2 in the voltage range of 2.75 and 4.4 V. Inductively coupled plasma−mass spectroscopy (ICP−MS) was used to measure the extent of cobalt dissolution into the electrolyte (with 1 mL), after floating the charged cathodes for 12 days.

Results and Discussion

The composition of the thin-film $LiCoO_2$ cathodes deposited onto the Pt current collector was determined using ICP−AES to obtain the Li/Co ratio and AES to obtain the O/Co ratio. The Li/Co and O/Co ratios determined by ICP−AES and AES are ~1.15 and ~2.05, respectively. The deviation from the ideal $LiCoO_2$ stoichiometry probably originates from the presence of small amounts of Li_2O present in the films, which cannot be detected by XRD.[7]

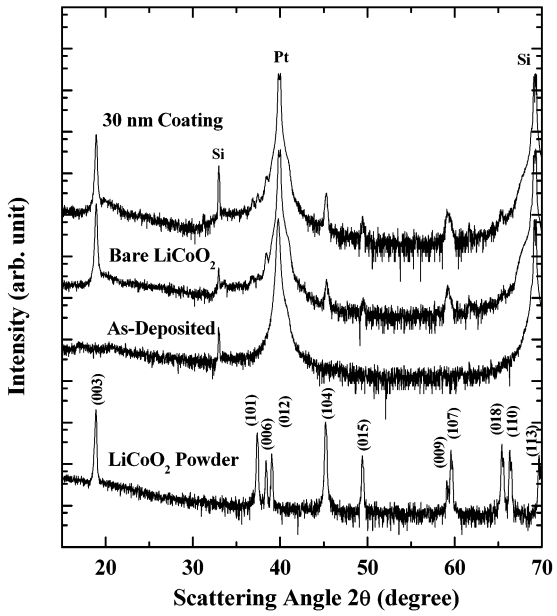

Figure 1. XRD patterns of a typical 30-nm-thick Al_2O_3-coated $LiCoO_2$ film, a bare $LiCoO_2$ film, an as-deposited $LiCoO_2$ film, and a $LiCoO_2$ powder, prior to cycling.

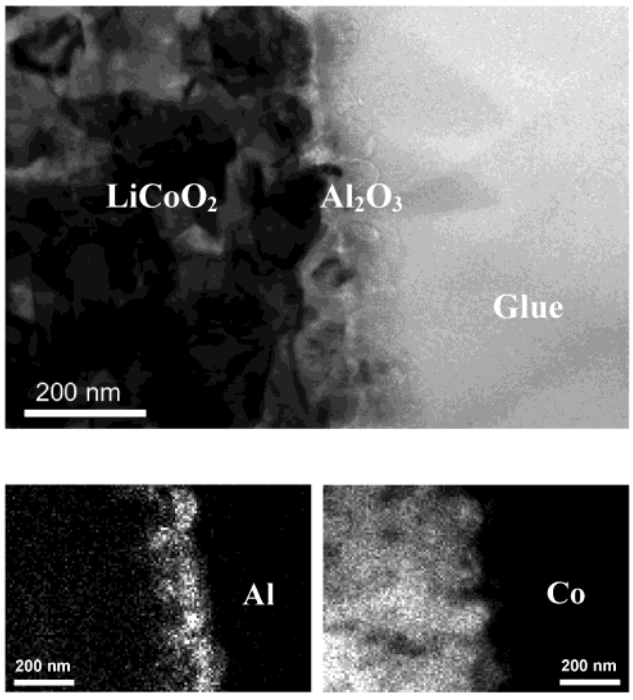

Figure 2. Cross-sectional TEM image and EDS mapping of an ~50 nm Al_2O_3-coated $LiCoO_2$ thin film.

In Figure 1, the XRD patterns of Al_2O_3-coated $LiCoO_2$ films are compared with the patterns of the $LiCoO_2$ powders and the bare $LiCoO_2$ thin film. The XRD patterns of the Al_2O_3-coated films do not show any peak corresponding to the Al_2O_3 phase, suggesting that the crystallinity of the Al_2O_3 layer may be poor. In addition, Figure 1 shows a crystallized $LiCoO_2$ thin film with a preferred (003) orientation of hexagonal $LiCoO_2$.

Figure 2 shows the cross-sectional TEM image of an Al_2O_3-coated $LiCoO_2$ with a continuous coating on top

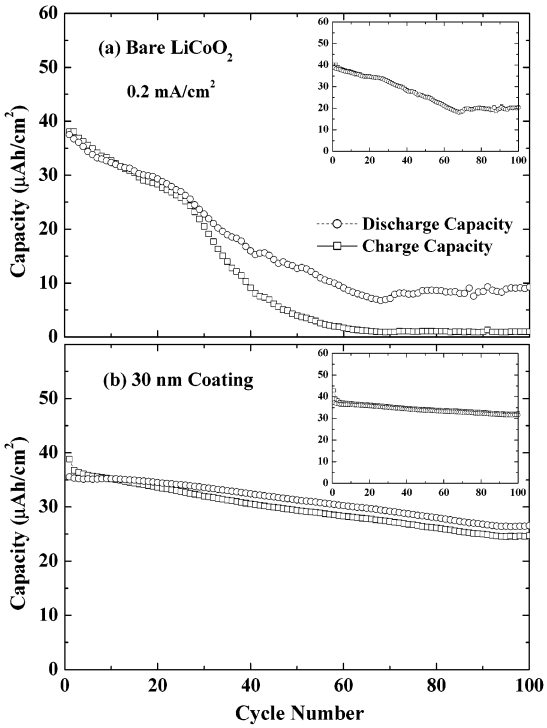

Figure 3. Cycle-life performance (charge and discharge capacities vs cycle number) of (a) bare, and (b) 30-nm-thick Al_2O_3-coated, $LiCoO_2$ thin films between 4.4 and 2.75 V at 0.2 mA/cm^2. The inset shows the same cycle-life performance, including the extra capacity from the constant-voltage mode.

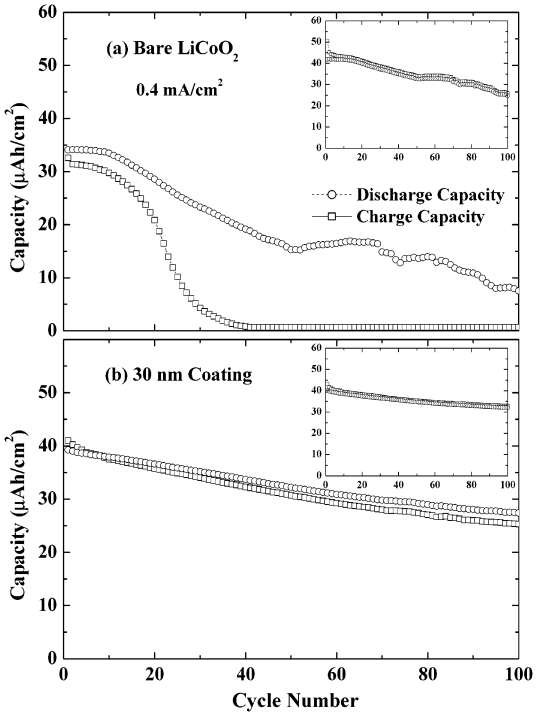

Figure 4. Cycle-life performance of (a) bare, and (b) 30-nm-thick Al_2O_3-coated, $LiCoO_2$ thin films between 4.4 and 2.75 V at 0.4 mA/cm^2. The inset shows the same cycle-life performance, including the extra capacity from the constant-voltage mode.

of the polycrystalline $LiCoO_2$ thin film. The EDS shows the Al components in the coating layer, indicating a sharp interface between an aluminum-oxide layer and $LiCoO_2$.

To test the cycle-life performance of the bare and 30-nm-thick Al_2O_3-coated $LiCoO_2$ thin films, half cells were cycled in the voltage range of 2.75 and 4.4 V at 0.2 and 0.4 mA/cm^2, as shown in Figures 3 and 4, respectively. A 30-nm-thick Al_2O_3 coating significantly improves the retention capacity of the $LiCoO_2$ thin-film cathodes. The charge and discharge capacities of the bare $LiCoO_2$ get deteriorated to only ∼3% and ∼25% of the original capacity after 100 cycles (Figure 3(a)), whereas those of the Al_2O_3-coated $LiCoO_2$ retain ∼64% and ∼75% of the initial capacity at a current rate of 0.2 mA/cm^2 (Figure 3(b)). The charge capacities of the bare $LiCoO_2$ films for Li deintercalation (charging) exhibit faster deterioration than the discharge capacities for Li intercalation (discharging). Nonlinearity of charge and discharge capacities in the uncoated samples may be related to the damage of $LiCoO_2$ (such as the surface corrosion) during the electrochemical cycling. We have recently reported that the effect of an Al_2O_3 coating on the cycle-life performance was more pronounced at the higher current rate (0.8 mA/cm^2).[17] The insets in Figures 3 and 4 show the same cycle-life performance, including the extra capacity from the constant voltage mode (at 4.4 and 2.75 V). In the bare samples, most of charge capacities after ∼40 cycles are attributed to the capacities at the constant voltage of 4.4 V, indicating that the Li deintercalation kinetics are slower than the Li intercalation kinetics. On the other hand, the Al_2O_3-coated samples show similar charge and discharge capacities, which is similar to the insets in Figures 3 and 4. This means that Li intercalation and deintercalation in the coated films become more symmetric. This clearly reveals that an Al_2O_3 coating modifies the properties of the cathode surface exposed to the electrolyte solution, and changes the Li-diffusion kinetics.

The Al_2O_3-coating thicknesses were varied from 10 to 300 nm to examine the possible questions of electronic insulation and Li migration through the Al_2O_3 layer. Figure 5(a) shows that the initial discharge capacities are almost independent of the coating thickness (0−300 nm range). In addition, the variation in the Al_2O_3 thickness ranging from 10 to 300 nm does not affect the capacity retention: ∼70% and ∼60% retention, respectively, at 0.2 and 0.4 mA/cm^2, whereas the capacity retention of the uncoated $LiCoO_2$ thin film is only ∼25% after 100 cycles, as shown in Figure 5(b). This is possibly because the Al_2O_3 coating layer acts as a solid electrolyte with a low electronic conductivity and a reasonably high Li-ion conductivity. For example, the Li-ion conductivity of a $Li_2O-Al_2O_3$ (0.7:0.3) solid electrolyte is $\sim 10^{-7}$ S/cm at room temperature.[23]

To clarify the reason the Al_2O_3-coated $LiCoO_2$ thin films showed better electrochemical performance than the bare ones, ICP−MS analysis was carried out after floating the films at 4.2, 4.4, 4.5, 4.6, and 4.7 V, respectively, for 12 days. As shown in Figure 6, the amount of cobalt dissolution from the uncoated $LiCoO_2$ films significantly increases with increasing charge-cutoff voltages, whereas an increase in cobalt dissolution from the Al_2O_3-coated ones is not significant. An increase in the fraction of Co^{4+} in $Li_{1-x}CoO_2$ augments the reactivity with the electrolytes and acidic HF in the

(23) Glass, A. M.; Nassau, K. *J. Appl. Phys.* **1980**, *51*, 3756.

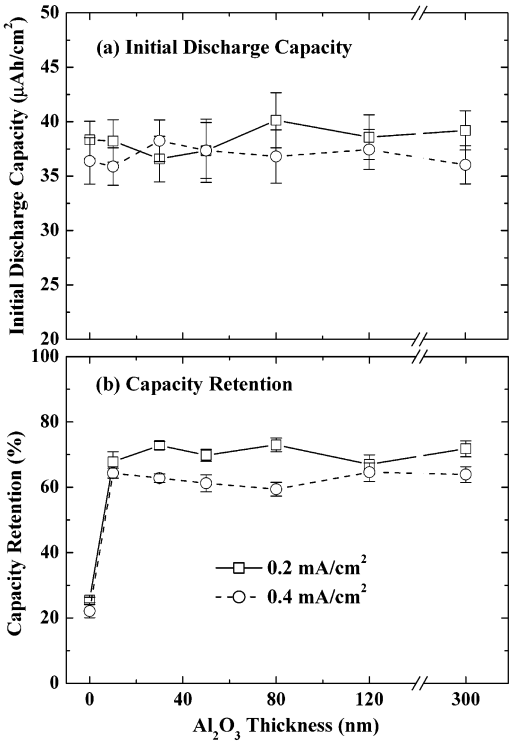

Figure 5. Effect of the Al_2O_3-coating thickness on the (a) initial discharge capacity, and (b) capacity retention after 100 cycles, all excluding the extra capacity from the constant-voltage mode. The cells were cycled between 4.4 and 2.75 V at 0.2 and 0.4 mA/cm^2.

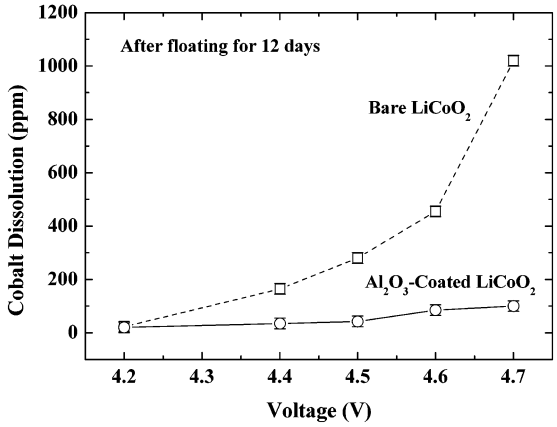

Figure 6. Amount of cobalt dissolution in the electrolyte (with 1 mL), from bare and Al_2O_3-coated $LiCoO_2$ after an initial charge, and being immersed for 12 days at 25 °C.

electrolyte. Amatucci et al.[4] reported that cobalt dissolution is closely related to a weakening of the crystal structure by the removal of the binding lithium. An Al_2O_3 coating can effectively inhibit cobalt dissolution even at 4.7 V (~100 ppm), which is much smaller than cobalt dissolution (~1000 ppm) from the uncoated $LiCoO_2$ films.

Figure 7 shows the changes in the lattice constants *c* as a function of the cell potential during the first charge in the $Li_{1-x}CoO_2$ thin films and powders.[18−20] Both the bare and Al_2O_3-coated $LiCoO_2$ thin films exhibit negligible *c*-axis expansion even with a preferred (003) orientation. This is in contrast to the $LiCoO_2$ powders, which exhibit ~2.6% *c*-axis expansion at ~4.17 V. Further studies are necessary to identify the mechanisms that cause $LiCoO_2$ thin films to have a limited *c*-axis expansion.

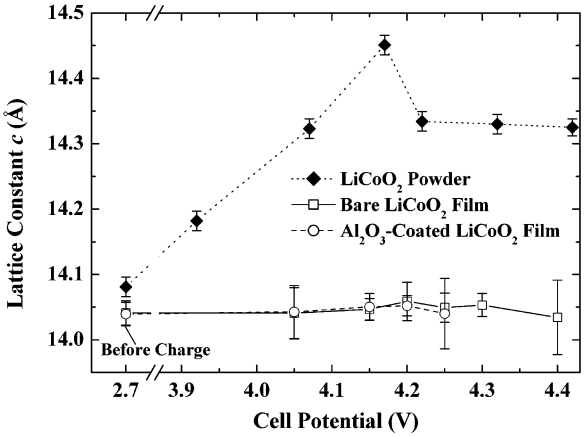

Figure 7. Changes in the lattice constants *c* as a function of the cell potential for bare and Al_2O_3-coated $LiCoO_2$ thin films during the first charge, and a comparison with powder samples.[18−20] For thin films, each cell was charged at a 0.1 mA/cm^2 rate to the predetermined voltages, then potentiostated until the current density decreased to 1 μA/cm^2.

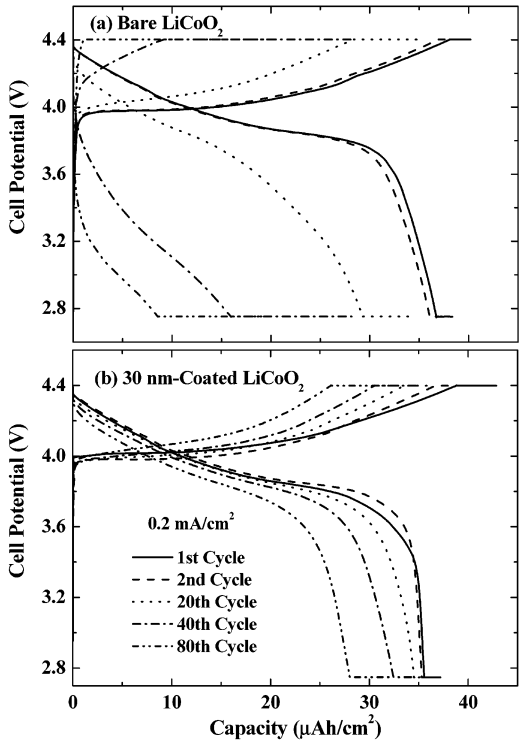

Figure 8. Voltage profiles of (a) bare, and (b) 30-nm-thick Al_2O_3-coated, $LiCoO_2$ films between 4.4 and 2.75 V at the rate of 0.2 mA/cm^2. At each charge/discharge cutoff step, the cell voltage was potentiostated until the current decreased to 0.02 mA/cm^2.

The voltage profiles of the bare and 30-nm-thick Al_2O_3-coated $LiCoO_2$ thin films are shown in Figure 8. The profiles of the bare $LiCoO_2$ thin films become steeper with increasing the cycling number up to 80 cycles at 0.2 mA/cm^2. In contrast, the change in the voltage profiles of the Al_2O_3-coated $LiCoO_2$ thin films during 80 cycles is more gradual. However, compared with the cycling profiles of bare $LiCoO_2$ thin films, the slight increase in cell potential is observed in the initial cycle of Al_2O_3-coated cathodes. This is attributed to the insulation of aluminum-oxide layer on the surface to the

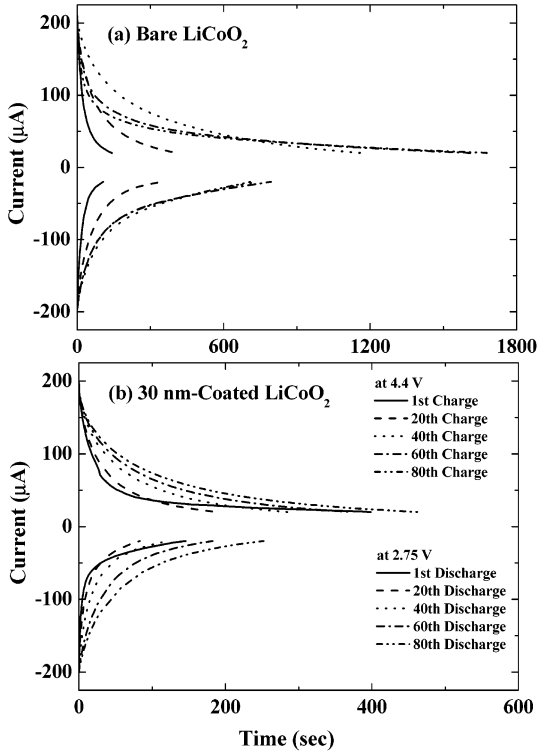

Figure 9. Current profiles during the constant voltages at 4.4 V (Li deintercalation) and 2.75 V (Li intercalation) with the current rates reduced from 0.2 mA/cm^2 to 0.02 mA/cm^2.

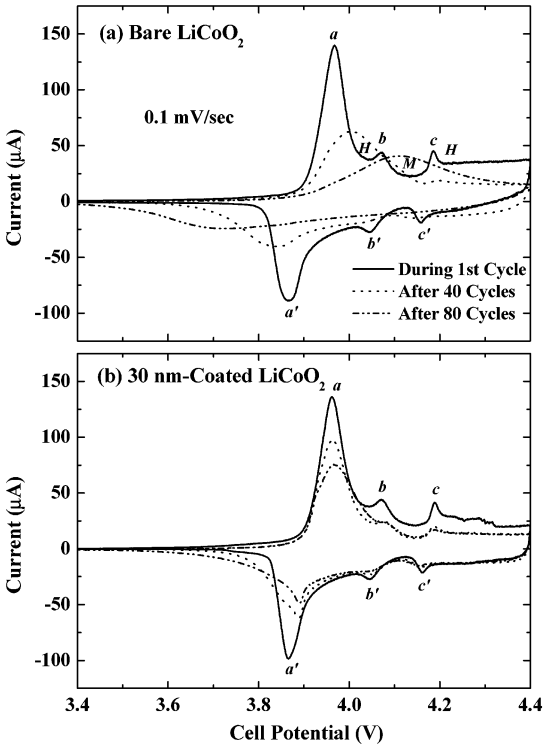

Figure 10. Cyclic voltammograms of (a) bare, and (b) 30-nm-thick Al_2O_3-coated, $LiCoO_2$ films after 0, 40, and 80 cycles. The sweep rate was 0.1 mV/sec between 3.0 and 4.4 V, and the symbols *H* and *M* indicate the hexagonal and monoclinic phases, respectively.

Li ions. From the second cycle on, the polarization in the charge and discharge processes of coated sample is not significant, which is because the Li−Al−O coating layer on the $LiCoO_2$ acts as a solid electrolyte as shown in Figure 5. Figure 9 shows the current profiles at a constant voltage of 4.4 V (Li deintercalation) and 2.75 V (Li intercalation) with the current rates reduced from 0.2 mA/cm^2 to 0.02 mA/cm^2 for decreasing the concentration gradient of Li in the cathode. The current profiles of the bare and Al_2O_3-coated $LiCoO_2$ films during the first cycling have similar decay constants. However, the currents of the Al_2O_3-coated $LiCoO_2$ films at the constant voltage of 4.4 and 2.75 V after the 80th cycle equilibrate more rapidly than those of the bare ones, due to the formation of a surface layer that can tolerate the electrochemical cycling with the high cutoff voltage.

Figure 10 shows the CVs of the bare and 30-nm-thick Al_2O_3-coated $LiCoO_2$ thin films at a scan rate of 0.1 mV/sec, which were carried out during the first cycle, and after the 40th and 80th charging/discharging cycles. The CVs of the Al_2O_3-coated $LiCoO_2$ thin films during the first cycle clearly show three sets of well-defined current peaks, i.e., the first set (∼3.96 and ∼3.87 V at *a* and *a*′), the second set (∼4.07 and ∼4.05 V at *b* and *b*′), and the third set (∼4.19 and ∼4.16 V at *c* and *c*′). The first set is due to the first-order phase transition between the two hexagonal phases, and the second and third sets are caused by the phase transition between the hexagonal and monoclinic phase.[1,2] These values are in good agreement with those obtained from the uncoated $LiCoO_2$ films and powders. However, these thin-film results are different from the CVs in the Al_2O_3-coated $LiCoO_2$ powders,[18,20] and the reasons for this disparity need to be identified. The cathodic peak (∼3.87 V at *a*′) of the Al_2O_3-coated film during the first cycle is narrower than that of the bare one, although the anodic peaks (∼3.96 V at *a*) are similar. In addition, in the bare $LiCoO_2$ thin films, the widths of both the cathodic and anodic peaks are remarkably broadened, and the peak positions become more separated as the number of cycles increases to 80, whereas the widths of the cathodic and anodic peaks of the Al_2O_3-coated samples are relatively sharp. This indicates that the Al_2O_3-coated $LiCoO_2$ thin films are more reversible than the bare ones, which is probably related to the suppression of cobalt dissolution from the cathode (Figure 6).

The effect of the Al_2O_3 coating on the Li intercalation/deintercalation kinetics during cycling was investigated by GITT, which is typically used for estimating the diffusivities of Li intercalation electrodes.[12,15,24−28] In GITT, the sample is subjected to a constant-flux lithiation or delithiation, which is interrupted after an interval τ, to allow the cell voltage to relax to its steady-state value. The temporary change in the cell potential caused by an outer current pulse allows the Li diffusivity to be determined. In this technique, the $Li_{1-x}CoO_2$ thin films were subjected to a constant-flux lithiation or delithiation (0.4 mA/cm^2) step. Sets of current pulses with an interval time τ = 10 s were applied, and the

(24) Weppner, W.; Huggins, R. A. *J. Electrochem. Soc.* **1977**, *124*, 1569.
(25) Hong, J.-S.; Selman, J. R. *J. Electrochem. Soc.* **2000**, *147*, 3190.
(26) Birke, P.; Chu, W. F.; Weppner, W. *Solid State Ionics* **1997**, *93*, 1.
(27) Levi, M. D.; Gamolsky, K.; Aurbach, D.; Heider, U.; Oesten, R. *J. Electroanal. Chem.* **1999**, *477*, 32.
(28) Choi, Y.-M.; Pyun, S.-I.; Bae, J.-S.; Moon, S.-I. *J. Power Sources* **1995**, *56*, 25.

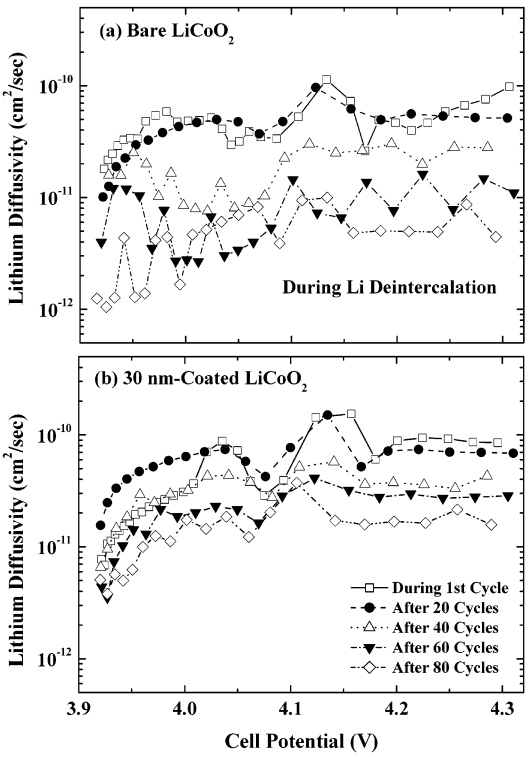

Figure 11. Lithium diffusivities as a function of the cell potential for (a) bare, and (b) 30-nm-thick Al_2O_3-coated, $LiCoO_2$ thin films determined by GITT during Li deintercalation (charging).

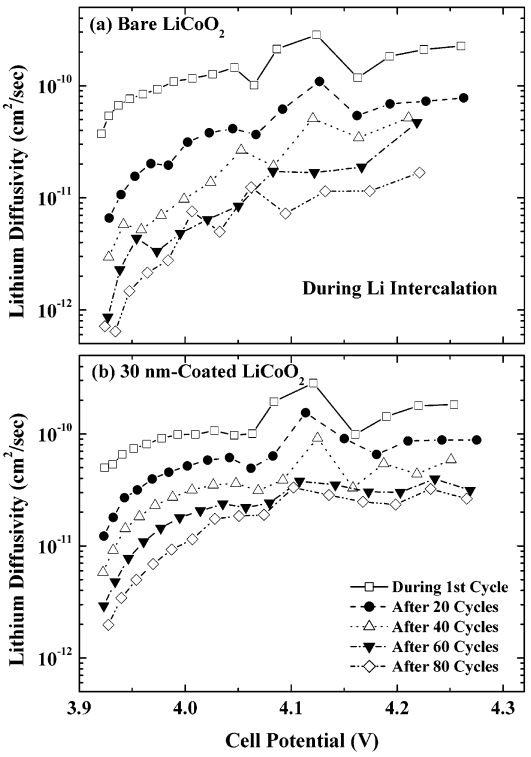

Figure 12. Lithium diffusivities as a function of the cell potential for (a) bare, and (b) 30-nm-thick Al_2O_3-coated, $LiCoO_2$ thin films, determined by GITT during Li intercalation (discharging).

current was interrupted for 10 min after each current pulse of 10 s. Weppner and Huggins[24] derived a simple expression for Li diffusivity in a thin film of intercalation electrode

$$\tilde{D}_{\mathrm{Li}} = \frac{4L^2}{\pi\tau}\left[\frac{\Delta E_s}{\Delta E_\tau}\right]^2 \text{ with } \tau \ll \tau_c \equiv \frac{L^2}{\tilde{D}_{\mathrm{Li}}} \qquad (1)$$

where L represents the film thickness of the $LiCoO_2$ cathode, and ΔE_τ and ΔE_s are the voltage changes during the current pulse and after the current pulse, respectively. The ideal density for the $LiCoO_2$ thin film was used for utilizing this equation.

Figures 11 and 12 show the apparent Li diffusivities as a function of the cell potential of the $Li_{1-x}CoO_2$ cathodes during Li deintercalation (charging) and intercalation (discharging), respectively. The Li diffusivities of Al_2O_3-coated $LiCoO_2$ are slightly lower than those of the bare one during the first Li deintercalation, as shown in Figure 11. The Li diffusivities in the bare $LiCoO_2$ thin films during Li deintercalation (Figure 11) are in good agreement with the previous results obtained using either thin-film $Li_{1-x}CoO_2$ cathodes[7,10,12,29] or powder electrodes.[25,27,28,30] Note that the plots of the Li diffusivity vs the cell potential show a maxima at ~4.13 V, corresponding to the monoclinic phase. In addition, two minima are observed at the cell potential corresponding to the phase transition between the hexagonal and monoclinic phase, which is similar to the previous reports by Jang et al.[10]

As the cycling number increases, the Li diffusivity decreases owing to the degradation of the thin-film $LiCoO_2$ cathodes. As shown in Figure 11, during Li deintercalation (charging), the Li diffusivities of the bare $LiCoO_2$ thin films (in the range of approximately 4.15 and 4.3 V) decrease to $\sim 5 \times 10^{-12}$ cm^2/sec after 80 cycles, compared to $\sim 2 \times 10^{-11}$ cm^2/sec in the coated films. During Li intercalation (discharging), the Li diffusivities in bare samples are $\sim 1 \times 10^{-11}$ cm^2/sec after 80 cycles, while the deterioration in the Li diffusivities in the coated ones remains at $\sim 3 \times 10^{-11}$ cm^2/sec (Figure 12). These results suggest that an Al_2O_3 coating on the $LiCoO_2$ thin films can tolerate the electrochemical cycling with a high cutoff voltage of 4.4 V, which is attributed to the suppression of cobalt dissolution by Al_2O_3 coating.

Further studies are currently underway to detail the microstructures of the Li−Al−O coating layer, and electric-potential distribution near the interface between the $LiCoO_2$ cathode and the Li−Al−O coating layer. In addition, the effect of Al_2O_3 coating on the oxidative decomposition of the electrolyte solution on the cathode surface needs to be identified.

Conclusions

The galvanostatic charge−discharge experiments showed that the cycle-life performance of the $LiCoO_2$ thin films was significantly improved by an Al_2O_3-surface coating. These results correlate well with the suppression of cobalt dissolution during electrochemical cycling in the Al_2O_3-coated $LiCoO_2$ thin films. Both the CVs and GITT results clearly showed that the Al_2O_3-

(29) McGraw, J. M.; Bahn, C. S.; Parilla, P. A.; Perkins, J. D.; Readey, D. W.; Ginley, D. S. *Electrochim. Acta* **1999**, *45*, 187.
(30) Aurbach, D.; Levi, D. L.; Levi, E.; Teller, H.; Markovsky, B.; Salitra, G. *J. Electrochem. Soc.* **1998**, *145*, 3024.

coated samples had higher Li diffusivities after 80 cycles than the bare samples. In addition, the Al_2O_3 thickness up to 300 nm did not affect the capacity retention and initial capacities. Therefore, an aluminum-oxide solid electrolyte can modify the properties of the cathode surface, by residing between the $LiCoO_2$ cathode and the liquid electrolyte, which can enhance the electrochemical stability.

Acknowledgment. This work was supported by the Center for Nanostructured Materials Technology under the 21C Frontier Programs of the Ministry of Science and Technology, and by KOSEF through the Research Center for Energy Conversion and Storage at Seoul National University. We thank Ki-Bum Kim for providing the vacuum-furnace system.

CM0201403